

to the electrical properties of the upper frozen layer. The conducting active layer, which is always present in the summer and hampers such galvanic methods as d-c resistivity measurements (10), had essentially no effect on the data obtained.

ANDREW KOZIAR

Department of Physics,  
University of Toronto,  
Toronto, Ontario, Canada M5S 1A7

D. W. STRANGWAY

Department of Geology,  
University of Toronto

#### References and Notes

1. P. Hoekstra and D. McNeill, in *North American Contribution to the Second International Conference on Permafrost* (National Research Council-National Academy of Sciences, Washington, D.C., 1973), pp. 517-526.
2. L. Cagniard, *Geophysics* **18**, 605 (1953). The scalar apparent resistivity is defined as

$$\rho_a = \frac{1}{\omega\mu_0} \left| \frac{E_x}{H_y} \right|^2$$

where  $\omega$  is angular frequency,  $\mu_0$  is the permeability of free space,  $E_x$  is electric field strength, and  $H_y$  is orthogonal magnetic field strength.

3. D. W. Strangway, C. Swift, R. Holmer, *ibid.* **38**, 1159 (1973).
4. The Involut Hill test site has been extensively studied and drilled by the Geological Survey of Canada.
5. The contouring program was obtained from Y. Lamontagne.
6. At the permafrost-half-space interface one would

determine that  $E_0 = (i\omega\mu_0\rho_2)^{1/2}H_0$ ,  $E_0$  and  $H_0$  being orthogonal. In the permafrost itself  $\nabla \times \mathbf{H} = 0$  and  $\nabla \times \mathbf{E} = i\omega\mu_0\mathbf{H}$ . At the surface of the permafrost it follows that  $H_y = H_0$  and  $E_x = [(i\omega\mu_0\rho_2)^{1/2} + i\omega\mu_0h]H_y$ , where  $h$  is permafrost thickness. Defining  $\rho_a$  as in (2) and  $\delta_2$  as in (7), it follows that

$$\rho_a = \rho_2 \left( 1 + \frac{2h}{\delta_2} + \frac{2h^2}{\delta_2^2} \right)$$

7. Skin depth,  $\delta_2 = (2\rho_2/\omega\mu_0)^{1/2}$ , is the depth at which a plane wave has been attenuated to  $e^{-1}$  of its initial amplitude.
8. The apparent resistivity curve begins to roll over when  $h \geq 0.2\delta_2$ , where  $\delta_2$  is the skin depth in the permafrost, or when  $\sigma t$ , the product of conductivity and thickness, exceeds 0.02 mho. The effect of displacement currents depends on  $\epsilon$ , which may be as high as  $100\epsilon_0$  for ice below  $10^4$  hertz ( $\epsilon_0$  is the electrical permittivity of free space). For the general expression of the surface impedance of a two-layer and three-layer earth, see J. R. Wait, *Electromagnetic Waves in Stratified Media* (Pergamon, New York, 1962).
9. The average over  $N$  stations is

$$\bar{\rho}_N = \frac{1}{N^2} \left[ \sum_{i=1}^N (\rho_i)^{1/2} \right]^2$$

10. D. F. Barnes and G. R. MacCarthy, *Preliminary Report on Tests of the Application of Geophysical Methods to Arctic Ground-Water Problems* (Open-file report, U.S. Geological Survey, Denver, Colo., 1964); A. A. Ogilvy, *Geol. Surv. Can. Econ. Geol. Rep. No. 26* (1970), pp. 641-648.
11. This work was primarily supported by the Canadian Defence Research Board while the author was under fellowship from the International Nickel Company; part of the equipment used was loaned by Kennecott Copper Corporation. Field support and logistics by W. J. Scott and the Geological Survey of Canada are gratefully acknowledged.

25 April 1975; revised 10 June 1975

## Neutron Diffraction Analysis of Myoglobin: Structure of the Carbon Monoxide Derivative

**Abstract.** *The locations of hydrogen and deuterium atoms and water molecules have been investigated in carbon monoxide myoglobin using neutron diffraction, and the results are compared with earlier work on metmyoglobin. Parallel real space refinements on the two molecules show relatively few changes, but do show the carbon monoxide molecule with the iron atom moving into the heme plane.*

Studies of sperm whale metmyoglobin (metMb) (1, 2) show that the positions of hydrogen atoms, deuterium atoms, and bound water molecules in a protein can be determined by neutron diffraction. In contrast to x-ray scattering factors, the neutron scattering length of the hydrogen atom is negative, and large enough to be seen readily in a Fourier synthesis. In this report we describe a neutron diffraction analysis of carbon monoxide myoglobin (MbCO), a low-spin derivative.

According to Perutz (3), mammalian hemoglobin (Hb) undergoes significant structural changes on transition to the low-spin case. X-ray comparisons of Mb derivatives of high (4), intermediate (5), and low (6, 7) spin do not show such large changes, although pH-dependent differences occur in

alkaline metMb (8). Hoard's prediction (9) that the low-spin ferrous iron is coplanar with the porphyrin [as observed for some porphyrin complexes (10)] has not been confirmed in any of these Mb studies. On the other hand, investigations of several



Fig. 1. Section of the MbCO neutron Fourier maps, showing CD4 phenylalanine. The side chain is well formed and indications of hydrogen atoms appear as negative contours.

Hb monomers (11-13) show structural changes with the iron in the heme plane. Neutron analysis allows examination of some of these questions, as well as the elucidation of the general hydrogen bonding, hydrogen-deuterium exchange, and the bound water structure.

A large crystal of MbCO (27 mm<sup>3</sup>) was grown from a 70 percent saturated ammonium sulfate solution at pH 5.7. The hydrogen atoms in the solvent (and thus in the water of hydration) were replaced with deuterium atoms after the crystal was grown, so as to reduce the background radiation resulting from the large incoherent neutron scattering of hydrogen. A neutron flux of  $1.0 \times 10^7$  neutrons per square centimeter per second was obtained at 1.52 Å with a pyrolytic graphite monochromator. An identical crystal served as analyzer to reduce half-wavelength contamination and background. Counting statistics were improved compared to those in the metMb work by the higher reflectivity of pyrolytic graphite and longer exposure times. Over 14,000 reflections in the 1.8 Å half-sphere were measured by rotating the crystal in 0.06° steps with a four-circle diffractometer at the Brookhaven High Flux Beam Reactor. After background and Lorentz corrections, absorption corrections were applied using the experimentally determined value of the neutron absorption coefficient,  $\mu = 2.4 \text{ cm}^{-1}$ . The agreement factor for the 6706 independent reflections was 3.8 percent in the structure factor,  $F$ .

Neutron phases were calculated from the Kendrew-Watson x-ray structure (14) (no hydrogen atoms). These calculated phases should approximate the true neutron phases in spite of the fact that omitting the hydrogen atoms leaves out almost half the total number of atoms in the protein. This is due to the systematic distribution of hydrogen atoms throughout the protein. Phase calculations on a model Mb structure show the average phase error due to the omission of hydrogen and deuterium atoms to be only 31° to a Bragg resolution of 1.8 Å. Further verification comes from the anomalous determination of several hundred phases from a Cd metMb derivative (15), where an average phase change of 37° was observed when compared to the calculated phases described above. The calculated phases are therefore sufficiently accurate for an analysis of the H, D, and D<sub>2</sub>O positions and for the initiation of a structure refinement.

Part of the MbCO Fourier map is depicted in Fig. 1, showing the CD4 phenylalanine side chain with evidence of hydrogen atoms that are bound to the aromatic ring. In general, the MbCO Fourier maps were clearer and less noisy than the metMb maps because of the larger data set and

better statistics. Both structures were refined by the real space technique (16) and compared to determine structural differences. This refinement minimizes the difference between the observed nuclear density and the model density as calculated from atomic coordinates. The details of the refinement on metMb (17) and MbCO have been presented recently (18). The refined values of the scattering length,  $b$ , for hydrogen atoms that cannot exchange give an indication of the validity of the final fit (see Table 1). For example, 98 percent of the  $C^\alpha$  hydrogen atoms were observed. On the other hand, values of  $b$  for hydrogen atoms that can exchange measure the hydrogen-deuterium exchange. As seen in Table 1, 64 percent of the main chain amides are observed to exchange, consistent with chemical studies (19, 20). One significant change in the hydrogen bonding between the two structures is evident at the ligand site. The proximity of various ligands to the  $N^{\epsilon 2}$  atom of the distal histidine imidazole ring has led several investigators (5, 11, 21–23) to suggest the existence of a hydrogen bond between them. The neutron maps show a deuterium bond here in metMb with  $D_2O$  at the ligand position (2, 17); however, no hydrogen or deuterium bond is found in MbCO. The hydrogen bonding of threonine and serine side chains to the main chain carbonyls was similar to that found in metMb. In general, the observed hydrogen and deuterium atom locations in MbCO are the same as in metMb.

Ordered water molecules and counterions were found in MbCO, as in metMb, on the protein surface near polar groups. One large and still unexplained peak was found in both metMb and MbCO deep in the hydrophobic pocket near the heme, serine G9, leucine H11, leucine E15, and isoleucine G12. In both metMb and MbCO, four water or counterion molecules form deuterium bonds to the propionic side chains of the porphyrin ring. Stereochemically they appear to hinder a ligand molecule entering or leaving the Mb molecule on the distal histidine side of the heme. This is consistent with work by Frauenfelder and co-workers (24), who examined MbCO by flash photolysis and found that the CO molecule can move out of the hydrophobic pocket, but is unable to leave the Mb molecule completely at low temperatures. Although we find no sign of a deuterium bond between the  $N^{\epsilon 2}$  atom of histidine FG3 and the nearest propionic side chain in either metMb or MbCO, there is a solvent bridge from  $N^{\delta 1}$  to the other propionic side chain.

Several changes in the tertiary structure of MbCO were found in the heme region, shown in Fig. 2. The view is along the  $c$ -axis and parallel to the heme. The crosses

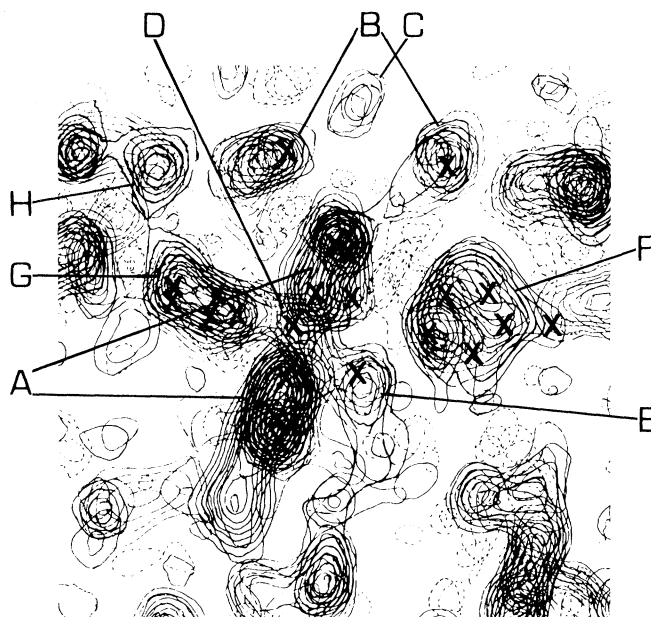


Fig. 2. View of the heme group environment. The porphyrin ring is the elongated density in the center. The following letters identify atomic groups or atoms: (A) porphyrin ring, (B) propionic side chains, (C)  $D_2O$  molecule, (D) iron, (E) CO molecule, (F) distal histidine E7, (G) proximal histidine F8, and (H) serine F7. The crosses represent the metMb x-ray coordinates. Note the lack of a deuterium bond from the CO molecule to the distal histidine. Below the CO molecule is a heme vinyl group. The valine E11 side chain is not shown in this section.

designate the metMb coordinates, which were used in the calculations of the neutron phases for the MbCO Fourier maps. The iron atom is in the center of the heme, with the proximal histidine on the left and the distal histidine on the right. Near the upper part of the density representing the heme are two peaks corresponding to part of each propionic side chain with a solvent molecule between them. The CO molecule is the elongated density on the distal histidine side and extending down into the hydrophobic pocket located about 0.8 Å below the axis linking the heme-linked histidine with the iron atom; the Fe–C–O bond angle is 135°. [Spectroscopic studies (23) indicate that the carbon atom binds to iron; neutron experiments do not distinguish carbon from oxygen.] Refinements of the two structures show changes at the edge of the heme in the vicinity of the E

helix and also at both propionic and vinyl side groups, whose conformational angles differ by about 10°. Movement of the heme interior, however, is less than 0.1 Å. The iron atom has moved over 0.3 Å closer to the heme in MbCO relative to metMb and is found about 0.1 Å from the plane of the four porphyrin nitrogen atoms. The EF corner of the polypeptide chain moves away from the heme; the valine E11 side chain has moved away from the ligand in MbCO as predicted by nuclear magnetic resonance work (25) and as observed in CO erythrocyruorin (12).

Atomic coordinates for all protein atoms, as well as water molecules, will be presented elsewhere (26).

JOHN C. NORVELL\*  
ANTHONY C. NUNEST†  
BENNO P. SCHOENBORN

Biology Department,  
Brookhaven National Laboratory,  
Upton, New York 11973

#### References and Notes

1. B. P. Schoenborn, *Nature (Lond.)* **224**, 143 (1969).
2. ———, *Cold Spring Harbor Symp. Quant. Biol.* **36**, 569 (1971).
3. M. F. Perutz, *Nature (Lond.)* **228**, 726 (1970).
4. J. C. Kendrew, *Science* **139**, 1259 (1963).
5. L. Stryer, J. C. Kendrew, H. C. Watson, *J. Mol. Biol.* **8**, 96 (1964).
6. H. C. Watson and B. Chance, in *Hemes and Hemoproteins*, B. Chance, R. Estabrook, T. Yonetani, Eds. (Academic Press, New York, 1966), p. 149.
7. H. C. Watson and C. L. Nobbs, in *Colloquium der Gesellschaft für Biologische Chemie* (Springer-Verlag, Berlin, 1968), p. 37.
8. B. P. Schoenborn, *J. Mol. Biol.* **45**, 297 (1969).
9. J. L. Hoard, *Science* **174**, 1295 (1971).
10. J. P. Collman, R. R. Gagne, C. A. Reed, W. T. Robinson, G. A. Rodley, *Proc. Natl. Acad. Sci. U.S.A.* **71**, 1326 (1974).
11. W. A. Hendrickson and W. E. Love, *Nat. New Biol.* **232**, 197 (1971).
12. R. Huber, O. Epp, H. Formanek, *J. Mol. Biol.* **52**, 349 (1970).
13. E. A. Padlan and W. E. Love, *J. Biol. Chem.* **249**, 4067 (1974).
14. H. C. Watson, *Prog. Stereochem.* **4**, 299 (1968).
15. B. P. Schoenborn, in *Proceedings of a Conference on Anomalous Scattering*, S. Ramaseshan and S.

Table 1. Presence of hydrogen or deuterium atoms for different groups as determined by the real space refinement. Main chain amides with zero density represent partial exchange. Hydrogen atoms should not exchange in the first four groups; they should exchange for deuterium in the last four groups, except in the hydrophobic pocket.

Atomic group	Hydrogen or deuterium atoms found
CH <sub>3</sub> (methyl)	79% H
CH <sub>2</sub> (hydrocarbon chain)	85% H
CH (planar ring)	88% H
C <sup>α</sup> H (main chain C <sup>α</sup> )	98% H
ND <sub>2</sub> (amide)	77% D
OD (hydroxyl)	100% D
ND <sub>3</sub> (ammonium)	80% D
ND (main chain amide)	25% H
	11% Zero density
	64% D

- C. Abrahams, Eds. (Munksgaard, Copenhagen, 1975).
16. R. Diamond, *Acta Crystallogr. Sect. A* **27**, 436 (1971).
  17. B. P. Schoenborn and R. Diamond, *Brookhaven Symp. Biol.*, in press.
  18. J. C. Norvell and B. P. Schoenborn, *ibid.*, in press.
  19. S. W. Englander and R. Staley, *J. Mol. Biol.* **45**, 277 (1969).
  20. H. I. Abrash, *C. R. Trav. Lab. Carlsberg* **37**, 107 (1970); *ibid.*, p. 129.
  21. P. A. Bretscher, thesis, Cambridge University (1968).
  22. L. Pauling, *Nature (Lond.)* **203**, 182 (1964).
  23. E. Antonini and M. Brunori, *Hemoglobin and Myoglobin in Their Reactions with Ligands* (North-Holland, Amsterdam, 1970).
  24. H. Frauenfelder, personal communication.
  25. R. G. Shulman, K. Wüthrich, T. Yamane, D. J. Patel, W. E. Blumberg, *J. Mol. Biol.* **53**, 143 (1970).
  26. B. P. Schoenborn, G. Darling, J. C. Norvell, in preparation.
  27. Research was carried out at Brookhaven National Laboratory, Upton, N.Y., under the auspices of the Energy Research and Development Administration.
- \* Present address: Laboratory of Molecular Biology, National Institute of Arthritis, Metabolism, and Digestive Diseases, National Institutes of Health, Bethesda, Md. 20014.
- † Present address: Institut Laue-Langevin, B.P. 156, Centre de Tri, 38042 Grenoble, France.

30 July 1975

## Aerosol Chemical Parameters and Air Mass Character in the St. Louis Region

**Abstract.** Comparisons of the chemical character of ambient aerosols in St. Louis during the month of September 1973 with the trajectory of the air parcel before it arrived in St. Louis indicate that regional sulfuric acid-ammonium bisulfate aerosol was associated with maritime tropical air and that regional ammonium sulfate aerosol was associated with continental polar air.

Recently reports have appeared indicating that  $\text{H}_2\text{SO}_4\text{-NH}_4\text{HSO}_4$  and  $(\text{NH}_4)_2\text{SO}_4$  were the optically dominant submicrometer aerosols in the St. Louis, Missouri, area during September 1973 (1). Further analysis of the data indicates that the occurrence of acidity ( $\text{H}_2\text{SO}_4\text{-NH}_4\text{HSO}_4$ ) is associated with maritime tropical air and the occurrence of salt [ $(\text{NH}_4)_2\text{SO}_4$ ] with continental polar air.

The University of Washington participated in the September 1973 preliminary Regional Air Pollution Study at St. Louis. The objective of the University of Washington team was to characterize the light-scattering properties of the aerosol and to measure the aerosol light-scattering as a function of relative humidity. A plot of light-scattering versus relative humidity is termed a "humidogram." In addition to indicating the hygroscopic nature of the aerosol, the humidogram can also provide information about the molecular or ionic composition of the aerosol (2).

For the period 4 to 27 September 1973, 99 percent of the humidograms of the aerosol at Tyson, Missouri (about 25 km west-southwest of St. Louis), exhibited either a monotonic, hygroscopic response or a deliquescent response with the deliques-

cent point at about 79 percent relative humidity. Data from 21 to 27 September (1) suggest that the hygroscopic humidograms consistently result from an aerosol containing a large fraction of acid as  $\text{NH}_4\text{HSO}_4$  or  $\text{H}_2\text{SO}_4$ . The observed deliquescent point in the remaining humidograms identifies the aerosol as containing a large fraction of salt as  $(\text{NH}_4)_2\text{SO}_4$ .

In the data analysis a concentrated effort has been made to discover variables that are related to this difference in the aerosols. One variable examined was the aerosol history. Ninety air parcel trajectories terminating at St. Louis for the average flow in the 500- to 2000-m layer were obtained from the National Oceanic and Atmospheric Administration (NOAA) Air Resources Laboratory (3). Examination of these trajectories revealed that 63 percent of the air parcels arriving from the south contained  $\text{H}_2\text{SO}_4\text{-NH}_4\text{HSO}_4$  aerosols, whereas 66 percent of the air parcels arriving from the north contained  $(\text{NH}_4)_2\text{SO}_4$  aerosol. This finding indicates that acid aerosols predominate in maritime tropical air masses whereas  $(\text{NH}_4)_2\text{SO}_4$  aerosol predominates in air masses of continental polar origin. To further examine this relationship, we plotted

coincidentally the percentage of the time during each day that the aerosol was  $(\text{NH}_4)_2\text{SO}_4$  as compared with the percentage of the time during each day that the air mass was continental polar, consulting the trajectories and 500-mbar charts (Fig. 1). The correlation coefficient between the 20 pairs of data points is 0.72 with a probability of less than 0.1 percent that this effect is due to random occurrence (4).

Although there is presently no model for a correlation of air mass and aerosol character, there are at least two possible causes for the observations reported here. First, there may be a lower  $\text{NH}_3$  source strength for air masses arriving at St. Louis after following marine tropical flow trajectories than for those arriving at St. Louis after following continental polar trajectories. This premise is supported by Junge's results (5) which show that the concentration of  $\text{NH}_4^+$  in precipitation for the midwestern states traversed by continental polar air masses is higher by as much as a factor of 10 than for the southeastern states traversed by marine tropical air masses. He suggests that the low  $\text{NH}_4^+$  concentration in the southeastern states may be due to the low pH value of yellowed laterite soils characteristic of the area. The second cause may be different aerosol production and modification processes for each air mass. Substantial differences in the thermal structure and moisture content of the two types of air mass suggest a variety of possible causal factors for the different aerosol character.

A. H. VANDERPOL, F. D. CARSEY  
D. S. COVERT, R. J. CHARLSON  
A. P. WAGGONER  
*Water and Air Resources Division,  
Civil Engineering Department, and  
Institute for Environmental Studies,  
University of Washington,  
Seattle 98195*

### References and Notes

1. R. J. Charlson, A. H. Vanderpol, D. S. Covert, A. P. Waggoner, N. C. Ahlquist, *Science* **184**, 156 (1974); *Atmos. Environ.* **8**, 1257 (1974).
2. D. Covert, thesis, University of Washington (1974).
3. J. Heffter, A. Taylor, G. Ferber, *A Regional-Continental Scale Transport, Diffusion, and Deposition Model* (publication NOAA TM ERL-50, National Oceanic and Atmospheric Administration Air Resources Laboratory, Silver Spring, Maryland, June 1975).
4. P. Bevington, *Data Reduction and Error Analysis for the Physical Sciences* (McGraw-Hill, New York, 1969), pp. 310-311.
5. C. Junge, *Air Chemistry and Radioactivity* (Academic Press, New York, 1963), figure 82, pp. 341-342.
6. We thank the staff of the NOAA Air Resources Laboratory, and in particular J. L. Heffter, for their cooperation in providing the air parcel trajectories used in our study. We also thank Prof. C. Junge for helpful discussions. This research has been supported from 1972 to the present by grants from the Environmental Protection Agency (present grant R800665) and the National Science Foundation (present grant DES 75-13922).

16 June 1975; revised 23 July 1975

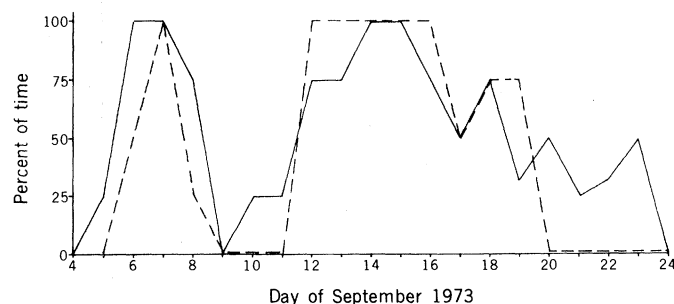


Fig. 1. Plot of the daily frequency of continental polar air masses in St. Louis (dashed line) with the daily frequency of  $(\text{NH}_4)_2\text{SO}_4$  aerosol (solid line) for September 1973.